

# The Optimization of Cam Profile – The Development of NEWCAM and MULTICAM Profile

Jurij Avsec<sup>1</sup>, Maks Oblak

*University of Maribor, Faculty of Mechanical Engineering,*

*Smetanova 17, 2000 Maribor, P.O. BOX 224, Slovenia*

<sup>1</sup>*jurij.avsec@uni-mb.si*

## 1. SUMMARY

This paper describes a new type of valve gear cams – MULTICAM – which consists of seven curves and allows an optimum cam profile design and NEWCAM – which consists of three curves. In order to calculate the cinematic and dynamic values and to assess the minimum oil film thickness in the valve gear, the mathematical model of an ideal valve gear was used. In addition, a comparison of the results between the polysine cam and the new MULTICAM cam design was made. By means of the new cam design the Hertz pressures were reduced at the point of contact between the cam and the cam follower and the lubrication properties at the top of the cam improved.

## 2. INTRODUCTION

The main task of the valve gear /1,2/ is control of the exhaust and inlet valve. In internal combustion engines the valve gear system has an important influence upon the power output and torque as well as on the exhaust gas emission. The forces required for the control are very high due to high accelerations occurring in the valve gear. Apart from the forces, wear and damage of the valve gear are also caused by the reactive reagents and high temperatures primarily on the exhaust side of the thermally loaded valve gear parts. The valve gear of truck and bus engines has undergone fast development in recent years. In Otto car engines the electro-hydraulic valve gear with variable valve gear design has been established in series production. It has an advantage over the conventional system primarily in the idling at lower engine loading /1/. In racing car engines, the pneumatic valve gear is already in use, due to a very fast response and the correspondingly very short valve opening and closing times. In truck and bus diesel engines only conventional valve gear designs are used in series production.

### 3. EXISTING VALVE GEAR

In our case, the engine durability test was carried out on a TAM BF 6L 515C diesel engine, incorporating a conventional valve gear. After the 3000-hour engine test the manifestations of intensive wear appeared on the exhaust side of the valve gear. The wear of the exhaust cam was especially intensive right under the top. This type of wear is called the surface wear and it occurs at low peripheral speeds, when the lubrication properties are weakened and high friction occurs between the cam and the follower when the side pressure is high. Both the inlet and exhaust cams in the test engine were designed in accordance with the polysine curve theory /2/. This type of cam is designed so as to yield a continuous acceleration curve.

### 4. VALVE GEAR DYNAMIC MODEL

In order to estimate the cam wear intensity and to compare the new cam designs with the existing ones a dynamic valve gear analysis was made. The real model of the real valve gear design can be written by means of the partial differential equations, the solution of which is a complex task. We used a simplified model with the following generalisations:

- 1) Entire system is rigid
- 2) Follower and push rod are in the axis of symmetry
- 3) Lift delay due to the cam follower inclination is ignored
- 4) Valve inclination in the second plane is ignored

The presented mathematical model gives applicable results primarily for medium- and low-speed internal combustion engines where our TAM BF 6L 515C is ranked. In such a case, the effects of elasticity and damping are not very high yet. Using the described simplifications, we calculated the contact forces between the valve gear elements:

$$F_3 = -(m_v + m_{kv} + 0.5m_{vz} + m_{vs})(g - a_v) + (F_L + k_v h_v) + + \frac{\pi}{4} D_v^2 p_g - \frac{\pi}{4} ((D_v^2 - d^2) p_c - d^2 p_0) \quad (1)$$

$$F_k = \left( F_3 l_1 \left( 1 + \frac{1}{i} \right) + J_k \epsilon + m_k g e - m_k g l_1 \right) \frac{1}{l_1 - \mu \frac{d_k}{2}} \quad (2)$$

$$F_2 = -F_3 + m_k g + F_k \quad (3)$$

$$F_l = F_2 + (m_p + m_s)(a_p + g) \quad (4)$$

In order to calculate the inertia forces we computed the reduced masses:

- a) On the side of the cam follower:

$$\text{In the zone of clearance: } m_{red_p} = m_p + m_s + J_k / l_1^2 \quad (5)$$

$$\text{Zone without clearance: } m_{red_p} = m_p + m_s + J_k / l_1^2 + (m_v + m_{vs} + m_{kv} + 0.5m_{vz}) / i^2 \quad (6)$$

b) On the side of valve:

$$\text{In the zone of clearance } m_{red_v} \approx 0 \quad (7)$$

$$\text{Zone without clearance: } m_{red_v} = (m_p + m_s)i^2 + J_k / l_2^2 + (m_v + m_{vs} + m_{kv} + 0.5m_{vz}) \quad (8)$$

At the same time we also took into account the effect of the shock force /9/ due to the dynamic influences of embedding of the cam follower by the valve opening:

$$a) \text{ On the side of the cam follower: } F_u = v_p \sqrt{m_{red_p} k_p} \quad (9)$$

$$b) \text{ On the side of the valve: } F_u = v_v \sqrt{m_{red_v} k_v} \quad (10)$$

By means of dynamic analysis we then carried out a review of values having a direct impact upon the valve gear wear:

- Control of Hertz pressures;
- Control of minimum oil film thickness according to elastohydrodynamic theory;
- Control of tangential stresses occurring some tenths of millimetres in the depth of the cam and being proportional to the normal tensions.

Tables 1 and 2 show the values of the highest Hertz pressure and the minimum oil film thickness occurring in the inlet and outlet cam at the idling (500 rpm of crankshaft) and at rpm exceeded by a 30% (2800 rpm of crankshaft), which can appear by vehicle moving downhill. In order to calculate the Hertz pressures we used the theory of rolling contacts [3,5,9]:

$$p_H (\text{N/mm}^2) = 0.418 \sqrt{\frac{F_1(N)E(N/\text{mm}^2)}{b_N(\text{mm})}} \left( \frac{1}{R_p(\text{mm})} + \frac{1}{RON(\text{mm})} \right) \quad (11)$$

$$RON = h_p + r_0 + \frac{a_p}{\omega^2} \quad (12)$$

$$E = \frac{2E_1E_2}{E_1 + E_2} \quad (13)$$

**Table 1**

Computation of normal tensions (Hertz pressures) at the top of the cam

| Crankshaft<br>Velocity (rpm) | Exhaust cam<br>(N/mm <sup>2</sup> ) | Inlet cam<br>(N/mm <sup>2</sup> ) |
|------------------------------|-------------------------------------|-----------------------------------|
| 500                          | 710                                 | 590                               |
| 2800                         | 560                                 | 480                               |

According to the sources from Reference /9/, the permissible Hertzian pressure loads are approximately 600 N/mm<sup>2</sup> /1,2/. As evident from Table 1, the loads are too high mainly on the exhaust cam. The minimum oil film thickness  $H_{min}$  was calculated using the elastohydrodynamic theory /[3,5/:

$$H_{min}(m) = 1.6 \cdot RON(m)^{0.43} \cdot \eta(Pas)^{0.2} \cdot |v_{HD}(m/s)|^{0.7} \cdot (F_1(N))^{-0.13} E(N/m^2)^{0.03} \quad (14)$$

$$v_{HD} = \left( r_0 + h_r + \frac{2a_p}{\omega^2} \right) \omega \quad (15)$$

The assessment of the minimum oil film thickness at the top of the exhaust cam (Table 2) does not provide any favourable results. As the largest loads appear at the top of the cam, where the highest wear was measured, it is necessary to reduce the normal tensions and improve the lubrication properties.

**Table 2**

Minimum oil film thickness at the top of the cam at 500 rpm

|           | Inlet system  | Exhaust system |
|-----------|---------------|----------------|
| $F_1$     | 1500 N        | 1100 N         |
| $V_{HD}$  | 1.2 m/s       | 1.0 m/s        |
| RON       | 5.6 mm        | 4.9 mm         |
| $H_{min}$ | 0.142 $\mu$ m | 0.1 $\mu$ m    |

Tables 1 and 2 show that the tensions at the top of the exhaust cam must primarily be lowered (SI1). This was achieved in two ways:

1. The design exhaust cam allows an increase in the base circle diameter from 41.6 mm to 45.6 mm. By means of a new base circle diameter we calculated the new optimum polysine cam design (NI1).
2. Through the use of the new MULTICAM and NEWCAM cam design. Due to the increase in the base circle we compared the new MULTICAM cam profile with the optimum one, which is designed in accordance with the polysine curve on the new base circle (NI2, NI3).

## 5. NEW MULTICAM AND NEWCAM CAM DESIGN

By using the dynamic model of the valve gear we analysed the causes of excessive wear. Since the cam (NI1), designed in accordance with the polysine curve, offered too few possibilities for an optimum cam profile, we wanted to manufacture a completely new type of cam with more possibilities for an optimum adjustment. At the same time, we wished to summarise some findings of authors on the dependence of the

cam design on the fuel consumption and valve gear noise. Thus, on this basis the new MULTICAM cam (NI2) was created.

By designing the new cam profile we wished to reduce the tensions primarily at the top of the cam without having to substantially change the other parameters. The following factors had to be taken into account:

1. We did not want to considerably change the basic characteristics of the cam (lift, angle of opening).
2. Excessive accelerations and changes in the speed of accelerations by cam follower lifting and lowering have to be avoided.
3. Geometrical cross sections of valves do not have to be substantially changed.
4. The position between the valve travel and piston around TDC has to be checked to prevent any contact in this area.
5. We did not want to change the layout and design solution of the valve gear.
6. We had to verify the intensity of the inertia and spring force due to potential interruption of the contact.

Contrary to the conventional theory of polysine cam, the motion in MULTICAM cam can be written by means of seven curves. Equations (16) to (22) present the lift of the cam in the vertical direction.

$$\text{Zone } 0 < \varphi_0 < \Phi_0: h_0 = -\frac{C_1}{2} \left( \frac{\Phi_0}{\pi} \right)^2 \cos \left( \frac{\varphi_0 \pi}{\Phi_0} \right) + \frac{C_1}{4} \varphi_0^2 + k_1 \varphi_0 + k_2 \quad (16)$$

$$\text{Zone } 0 < \varphi_1 < \Phi_1: h_1 = -\frac{C_2}{2} \left( \frac{\Phi_1}{\pi} \right)^2 \sin \left( \frac{\varphi_1 \pi}{\Phi_1} - \frac{\pi}{2} \right) + \frac{C_2}{4} \varphi_1^2 + k_3 \varphi_1 + k_4 \dots \quad (17)$$

$$\text{Zone } 0 < \varphi_2 < \Phi_2: h_2 = \frac{C_2}{2} \varphi_2^2 + k_5 \varphi_2 + k_6 \quad (18)$$

$$\text{Zone } 0 < \varphi_3 < \Phi_3: h_3 = \frac{C_2}{2} \varphi_3^2 - \frac{C_2}{12} \cdot \frac{\varphi_3^4}{\Phi_3^2} + k_7 \varphi_3 + k_8 \quad (19)$$

$$\text{Zone } 0 < \varphi_4 < \Phi_4: h_4 = \frac{C_2}{12} (\dot{\varphi}_4 - \varphi_4)^4 - C_5 \frac{\varphi_4^2}{2} + k_9 \varphi_4 + k_{10} \quad (20)$$

$$\text{Zone } 0 < \varphi_5 < \Phi_5: h_5 = -\frac{C_5}{2} \left( \frac{\varphi_5}{\pi} \right)^2 \sin \left( \frac{\pi \varphi_5}{\Phi_5} - \frac{\pi}{2} \right) - \frac{C_5}{4} \varphi_5^2 + k_{11} \varphi_5 + k_{12} \quad (21)$$

$$\text{Zone } 0 < \varphi_6 < \Phi_6: h_6 = C_6 + k_{13} \varphi_6 + k_{14} \quad (22)$$

The constants  $C_1-C_6$  and  $k_1-k_{14}$  in equations (16)-(22) were obtained by means of boundary conditions. The NEWCAM cam is presented with three curves and the following equations:

$$\text{Zone } 0 < \varphi_1 < \Phi_1: h_1 = C_1 \left( \frac{\varphi_1^4}{12} \right)^2 + a_{1r} \frac{\varphi_1^2}{2} + k_1 \varphi_1 \quad (23)$$

$$\text{Zone } 0 < \phi_2 < \Phi_2: h_2 = -\frac{C_2}{12} \left( \phi_2 - \frac{\Phi_2}{2} \right)^4 + a_{2m} \frac{\phi_2^2}{2} + k_3 \phi_2 + k_4 \quad (24)$$

$$\text{Zone } 0 < \phi_3 < \Phi_3: h_3 = \frac{C_2}{12} (\phi_3 - \Phi_3)^4 + a_{3m} \frac{\phi_3^2}{2} + k_5 \phi_3 + k_6 \quad (25)$$

The constants  $C_1-C_3$  and  $k_1-k_6$  in equations (23)-(25) were obtained by means of boundary conditions. After deep study of MULTICAM and NEWCAM cam design, we have decided to develop further the MULTICAM cam. In Table 3 we present two new versions of MULTICAM cams in comparison with the older version of polysine exhaust cam.

**Table 3**  
Optimum cam angles

| New cam profile     | POLYSINE<br>(NI1) | MULTICAM<br>(NI2) | MULTICAM<br>(NI3) |
|---------------------|-------------------|-------------------|-------------------|
| Full lift (H)       | 9 mm              | 9 mm              | 8.7 mm            |
| Ramp lift ( $H_0$ ) | 0.3 mm            | 0.3 mm            | 0.3 mm            |
| Half angle $\phi$   | 78°               | 80°               | 80°               |
| Angle $\phi_0$      | 12°               | 10°               | 10°               |
| Angle $\phi_1$      | 20°               | 4.5°              | 4.5°              |
| Angle $\phi_2$      | 7°                | 0.3°              | 0.3°              |
| Angle $\phi_3$      | 39°               | 15.5°             | 15.5°             |
| Angle $\phi_4$      |                   | 42°               | 42°               |
| Angle $\phi_5$      |                   | 7.4°              | 7.4°              |
| Angle $\phi_6$      |                   | 0.3°              | 0.3°              |

## 6. RESULTS AND DISCUSSION

The comparison of the cam profiles is given in Figs. 1 to 5 and they show the comparison of curvature of cam, Hertz pressures and the force on the contact between cam and cam follower. The analysis of bending radius provides more favourable results for the MULTICAM cam profile (version NI2), whereas the analysis of the  $F_1$  contact force indicates that the force is considerably lower at the top of the cams designed in accordance with the polysine curve. In Fig. 1 and Fig. 2, the Hertz pressures diagrams are shown, occurring at the point of contact between the cam and cam follower. By using the new NI2, NI3 cam profile the Hertz pressures were substantially reduced, namely by 400 N/mm<sup>2</sup>. The top of the cam is the least loaded with the MULTICAM curve shape. In spite of a higher contact force the normal tensions are lower with MULTICAM

cam mainly due to higher radius of cam curvature. On the basis of the dynamic analysis both newly designed cams show lower tensions at the top of the cam and better lubrication properties, whereas the flow geometrical cross sections and the other control values remain similar for the all three versions of cams. The inertia and spring force ratio indicates more favourable results for the MULTICAM cam design /10/.

In Figs. 1-5 curve 1 mean exhaust cam, 2-intake cam, 3-MULTIPOLE cam (NI2), 4-Polysine cam (NI1) and 5-MULTIPOLE cam (NI3)

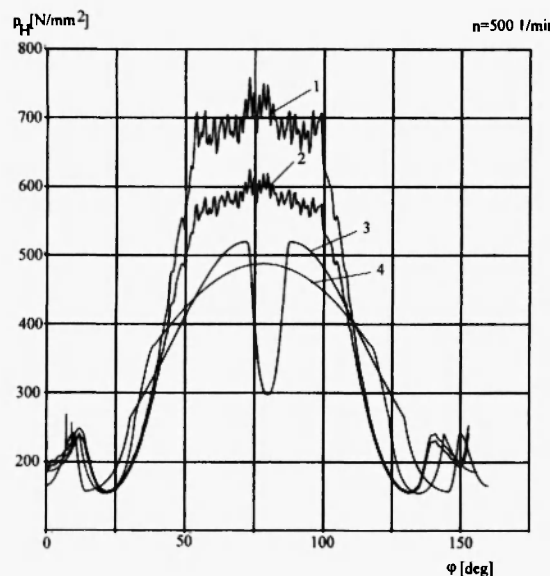


Fig. 1: Hertz pressures between cam and cam follower at 500 rpm of camshaft (at idling)

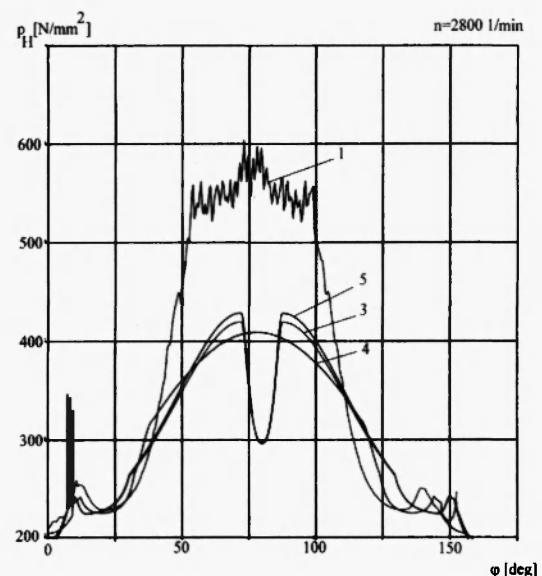


Fig. 2: Hertz pressures between cam and cam follower at 2800 rpm (exceeded by 30%)

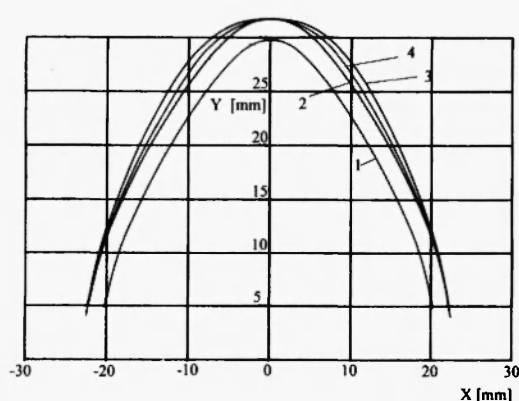


Fig. 3: Comparison of cam profiles

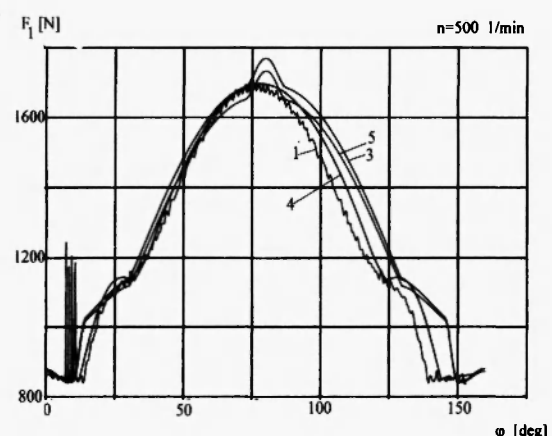


Fig. 4: Force at the contact between cam and cam follower at  $n=500$  rpm

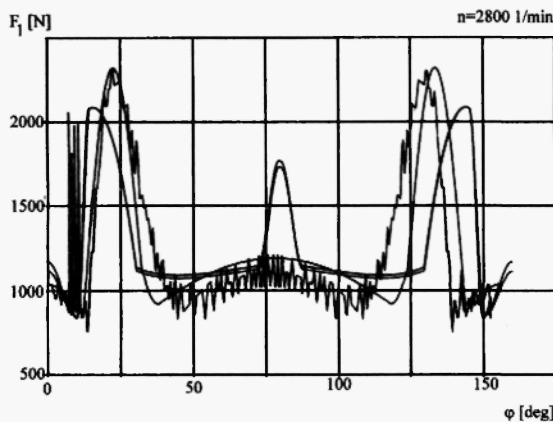


Fig. 5: Force at the contact between cam and cam follower at  $n=2600$  rpm

1-exhaust cam, 2-intake cam, 3-MULTIPOLE cam (NI2), 4-Polysine cam (NI1) 5-MULTIPOLE cam (NI3)

## 7. CONCLUSION

The design of diesel engine valve gear is often accompanied by a large number of complex problems, which have to be solved. In our case the problem was the intensive wear at the top of the exhaust cam profile after the 3000-h test on the engine. The choice of cam profile is a matter of primary significance in the procedure of valve gear design.

This paper describes our theoretical and practical contribution to the optimisation of valve gear design, including the ramp period. For these purpose we developed a new cams, called MULTICAM and NEWCAM, which consist from seven and three different curves. To estimate the kinematics, dynamical and lubrication properties with the new cam profile a simple mathematical model of valve gear was used.

With the new cam profile the Hertz pressure on the contact between cam and cam follower was reduced and also oil film thickness was improved. The calculation of other important values, as for example the ratio between inertia forces and spring forces, shows favourable results too.

## 8. REFERENCES

1. M. Kahrs, "Hydraulische Verstellungen für variable Ventiltriebe", *MTZ (Motortechnische Zeitschrift)* **56** (7/8), 413-417 (1995).
2. W. Bensinger, "Die Steuerung des Gaswechsels in schnelllaufenden Verbrennungsmotoren", Springer, Berlin, 1995.

3. G. Kümpel, "Anwendung der Elastohydrodynamik auf Nocken-Stössel Systeme", *Tribologie-Schmierungstechnik*, 33 (5), 299-308 (1986).
4. H. Kanesake, K. Ahila and H. Sahai, "A New Method of Valve Cam Design HYSDYNE CAM", SAE 770777.
5. B.P. Williamson and J.C. Bell, "The Effects of Engine Oil Rheology on the Oil Film Thickness and Wear Between a Cam and Rocker Follower", SAE 962031.
6. G.W. Stochowiak and A.W. Batchelor, "Engineering Tribology", Elsevier, Amsterdam, 1993.
7. H. Hardenberg, "Die Berechnung des freien Öffnungquerschnittes von Kegelventileen", *MTZ*, 30 (2), 59-64 (1969)..
8. "Die Verbrennungsentwicklung der neuen Mercedes-Benz Nutzfahrzeug, Dieselmotoren OM 442A und OM 442LA", *ATZ (Automobiltechnische Zeitschrift)*, 98 (2), 23-54 (1998).
9. V. Küntscher, "Kraftfahrzeugmotoren", VEB Verlag Technik Berlin, 1987.
10. J. Avsec, M. Marcic and M. Oblak, "Valve gear refinement", *J. Mech. Design*, 124 (3), 86-90 (2001).

